Colloids and Surfaces B: Biointerfaces 102 (2013) 611–619

Contents lists available at SciVerse ScienceDirect

Colloids and Surfaces B: Biointerfaces

journal homepage: www.elsevier.com/locate/colsurfb

Diffusion of dissolved ions from wet silica sol–gel monoliths: Implications for biological encapsulation

David J. Dickson[a], Bethany Lassetter[b], Benjamin Glassy[b], Catherine J. Page[b], Alexandre F.T. Yokochi[c], Roger L. Ely[d,*]

[a] College of Earth, Ocean, and Atmospheric Sciences, Oregon State University, 104 CEOAS Administration Building, Corvallis, OR 97331, USA
[b] Department of Chemistry, 1253 University of Oregon, Eugene, OR 97403, USA
[c] Department of Chemical, Biological, and Environmental Engineering, Oregon State University, 102 Gleeson Hall, Corvallis, OR 97331, USA
[d] Department of Biological and Ecological Engineering, Oregon State University, 116 Gilmore Hall, Corvallis, OR 97331, USA

ARTICLE INFO

Article history:
Received 2 February 2012
Received in revised form 20 August 2012
Accepted 28 August 2012
Available online 10 September 2012

Keywords:
Silica sol–gel
Diffusion
Bioencapsulation
Tetraethoxysilane
Organically modified siloxane

ABSTRACT

Divalent nickel (Ni^{2+}), Cu(II)EDTA, methyl orange, and dichromate were used to investigate diffusion from hydrated silica sol–gel monoliths. The objective was to examine diffusion of compounds on a size regime relevant to supporting biological components encapsulated within silica gel prepared in a biologically compatible process space with no post-gelation treatments. With an initial sample set, gels prepared from tetraethoxysilane were explored in a factorial design with Ni^{2+} as the tracer, varying water content during hydrolysis, acid catalyst present during hydrolysis, and the final concentration of silica. A second sample set explored diffusion of all four tracers in gels prepared with aqueous silica precursors and a variety of organically modified siloxanes. Excluding six outliers which displayed significant syneresis, the mean diffusion constant (D_{gel}) across the entire process space of sample set 1 was 2.42×10^{-10} m^2 s^{-1}; approximately 24% of the diffusion coefficient of Ni^{2+} in unconfined aqueous solution. In sample set 2, the tracer size and not gel hydrophobicity was the primary determinant of changes in diffusion rates. A strong linear inverse correlation was found between tracer size and the magnitude of D_{gel}. Based on correlation with the tracers used in this investigation, the characteristic 1-h diffusion distance for carbonate species relevant to supporting active phototrophic organisms was approximately 1.5 mm. These results support the notion that silica sol–gel formulations may be optimized for a given biological entity of interest with manageable impact to the diffusion of small ions and molecules.

1. Introduction

Sol–gel derived silica is gaining interest as an attractive material for the encapsulation of biological components. The broad variety of applications, from bioreactors to biosensors to tissue therapy and drug delivery systems, has been the subject of many recent reviews [1–8]. Silica gel offers the ability to effectively encapsulate functional proteins and viable cells. The material is inert and stable compared to organic polymer alternatives, creating a stabilize platform for enzymatic or biological conversion of substrates, biosensing, or biomedical applications.

In many potential biological applications the transport of dissolved materials can be critically important for optimal performance of the encapsulated component. Once gelation has occurred, diffusion is the dominant transport mechanism. The structural features and surface chemistry of the gel can have a strong influence on diffusion, especially as the size of the diffusing species approaches the size of the pores in the gel [9,10]. The precursor composition and processing parameters can control the size distribution of the gel porosity to some degree [11–14], so therefore should provide the ability to exercise some control over diffusion rates of dissolved species within the gel.

Diffusion in condensed gels that have undergone post-gelation processing (aging, drying, solvent exchange and/or heat treatments) has been extensively studied [9,10,15,16], as have structural features [11]. However, these investigations have generally been performed in the context of separations, such as membrane filtration or chromatography [8,17], and frequently the post-gelation treatments are incompatible with biological components. Characterization of diffusion in wet gels that have received no post-gelation treatment has received comparatively less attention. This is due to both a lack of relevant applications until recently and the dearth of experimental techniques that allow direct examination of the structure of the gel at high resolution without supercritical drying or chemical modification, both of which fundamentally alter the gel structure.

* Corresponding author. Tel.: +1 541 737 9409; fax: +1 541 737 2082.
E-mail address: ely@engr.orst.edu (R.L. Ely).

0927-7765/$ – see front matter © 2012 Elsevier B.V. All rights reserved.
http://dx.doi.org/10.1016/j.colsurfb.2012.08.063

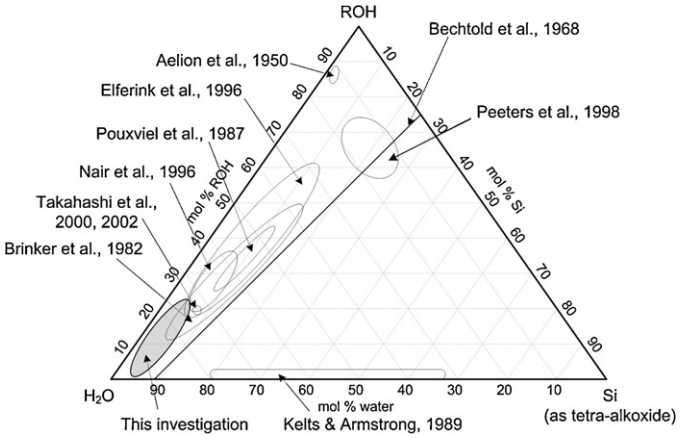

Fig. 1. Ternary phase diagram illustrating the process space for numerous investigations of sol–gel processed silica, including the present study.
Adapted from Brinker et al. [21].

In this study, we report the diffusion of dissolved ions from impregnated silica gels prepared via silicon alkoxide and sodium silicate (aqueous) sol–gel synthesis. Our interest lies in optimizing gels for the encapsulation of viable cyanobacteria as a platform for photobiological hydrogen production [18,19]. Although it has been claimed that virtually any microorganism that can be cultured can be encapsulated [2], it remains clear that the encapsulation process must be uniquely tailored to the organism of interest [4]. Therefore, the current investigation focuses on the effects that manipulating parameters in a processing space relevant to biological encapsulation (low silica, low alcohol, high water, and no cytotoxic post-gelation treatments) have on the diffusion of small molecules from bulk gel monoliths. The goal was to determine the processing space that allowed for maximum diffusion rates while maintaining adequate integrity and stability of the silica gel. The approximate process space selected for this investigation is shown graphically in the ternary phase diagram in Fig. 1. The parameters of previous investigations shown in Fig. 1 helped define the process space of the current work and provided fundamental descriptions of acid-catalyzed hydrolysis, base-catalyzed condensation, and polymerization prior to and during gelation [11,12,20–25]. However, prior investigations generally used supplemental alcohol as a co-solvent to prepare gels with relatively high silica content and performed post-gelation treatments (e.g. solvent exchange, annealing, etc.), reducing the relevance for biological encapsulation.

This investigation was conducted in two phases. First, divalent nickel, Ni^{2+}, was used as a tracer to probe diffusion from gel monoliths synthesized across a broad range of processing space. The parameters varied included the amount of water present during hydrolysis, the amount of acid catalyst present during hydrolysis, and the amount of silica present in the final gel (see Section 2). Ni^{2+} was selected because it is easy to measure the concentration with UV–Vis spectroscopy and it is similar in size to other dissolved ions and molecules that are of biological significance (e.g. CO_2 and bicarbonate) but not easily measured with UV–Vis spectroscopy.

Second, ions of differing size and charge were used to explore diffusion in a smaller process space, presumably most relevant to biological encapsulation. The selected ions included Ni^{2+}, methyl orange, ethylenediaminetetraacetic acid copper(II) disodium salt (Cu(II)EDTA), and potassium dichromate. These probes were selected for both their range of charge and size as well as ease of measurement with UV–Vis spectroscopy. Also included in this second phase was the incorporation of organically modified siloxanes (ORMOSILs) into the gels, including methyltriethoxysilane (MTES), dimethyldiethoxysilane (DMDES), trimethylethoxysilane (TMES), ethyltriethoxysilane (ETES), and propyltriethoxysilane (PTES). To varying degrees, these compounds introduce hydrophobicity to an otherwise hydrophilic gel, potentially altering the interaction with, and diffusion of the selected tracer molecules. It was the intent of the current study to determine how process space and the use of ORMOSILs may impact the bulk diffusion rates of molecules in a size regime comparable to compounds requisite for viable cyanobacterial cells.

2. Experimental methods

2.1. Materials

Gel precursors, including tetraethoxysilane (TEOS), ethyltriethoxysilane (ETES) (Alfa Aesar, Ward Hill, MA, or Gelest, Morrisville, PA), methyltriethoxysilane (MTES), dimethyldiethoxysilane (DMDES) (Sigma Aldrich, St. Louis, MO, or Gelest, Morrisville, PA), trimethylethoxysilane (TMES) (Tokyo Chemical Industry Co., Tokyo, Japan; and Gelest, Morrisville, PA), propyltriethoxysilane (PTES) (Gelest, Morrisville, PA), 40% sodium silicate (Na_2SiO_3) solution (aqueous precursor), nickel chloride hexahydrate (Fisher Scientific, Fair Lawn, NJ), ethylenediaminetetraacetic acid copper(II) disodium salt (Cu(II)EDTA), powdered methyl orange, and potassium dichromate (Sigma Aldrich, St. Louis, MO) were used as received. Additional reagents included potassium hydroxide (J.T. Baker, Phillipsburg, NJ) and nitric acid (Fisher Scientific, Pittsburgh, PA), both used as received to prepare 1.0 M stock solutions. Deionized water with a resistivity of 18.2 MΩ-cm was produced in house by reverse osmosis (Millipore Corp., Danvers, MA) and used for all gel solutions, stock solutions, and the preparation of buffered BG-11 medium [26] with 35 mM HEPES buffer (4-(2-Hydroxyethyl)piperazine-1-ethanesulfonic acid, N-(2-hydroxyethyl) piperazine-N′-(2-ethanesulfonic acid), an organic buffer used as received (Sigma Aldrich, St. Louis, MO).

2.2. Gel preparation

All of the alkoxide-derived gel samples were prepared with a two step process beginning with acid-catalyzed hydrolysis of the precursor to prepare a 'sol,' followed by base-catalyzed condensation. Base-catalyzed condensation was selected for two reasons: (1) for biological encapsulation, neutral pH is generally preferred, so using a base to neutralize the acidic sol served this purpose; and (2) base-catalyzed condensation yields a more highly condensed particulate structure, as opposed to acid-catalyzed condensation which tends to yield a network of linear polymers [33]. Firstly, a mixture of silicon alkoxide was hydrolyzed with varying amounts of nitric acid and deionized water. Secondly, buffered BG-11 medium [26] was added to catalyze gelation, containing a suitable concentration of potassium hydroxide to neutralize the acid catalyst and a tracer. All gels were prepared in 35 mm Petri dishes at a volume of 8.0 mL, filling the Petri dish and creating nearly ideal one-dimensional diffusion geometry. BG-11 was used over deionized water in sample preparation because it is typically used to grow cultures of the cyanobacterium *Synechocystis* sp. PCC 6803 (*Synechocystis*) for encapsulation studies [18,19]. Since BG-11 contains a variety of trace minerals and nutrients which may alter gelation kinetics, it was used in order to ensure the current investigation was directly applicable to on-going encapsulation studies. The amounts of water and acid used were determined based on gel formulation and the concentration of tracer was consistent for all samples prepared.

For the first phase of the investigation (sample set 1, using N^{2+} as a tracer), three parameters were varied over the following ranges:

1. The molar ratio of water to silicon alkoxide precursor in the initial hydrolysis (step 1), called the "hydrolysis ratio," was varied at 4:1, 10:1, and 20:1, water to silicon;
2. The molar ratio of nitric acid used to catalyze hydrolysis in step 1, or the "acid ratio," varied from 1:0.005 to 1:0.02, alkoxide to acid, at three increments, 0.005, 0.01, and 0.02; and
3. The final concentration of silicon during gelation (step 2), or the "dilution ratio," again expressed as a molar ratio of water to silicon, varied at 10:1, 20:1, 40:1, 60:1, 80:1, 100:1, and 120:1.

The range of these parameters was determined based on values relevant to designing gels for the encapsulation of living cells, consistent with prior experience [18,19], and the limits of gel samples able to be synthesized with this protocol. Sample set 1 used gels composed of TEOS only, in a factorial design to cover most combinations of parameters above in triplicate, resulting in 48 different sample types and 144 total samples.

Sample set 2 used limited gel formulations and multiple tracers to examine the effects of the size of the tracer and alterations to surface hydrophobicity, achieved by introducing ORMOSILs into the gel formulations. The hydrolysis and acid ratios were held constant through this sample set at 20:1 and 0.005, respectively, while a final dilution ratio of approximately 100:1 was maintained and 10 mol.% (percentage of total siloxane, with 90% TEOS) of MTES, DMDES, TMES, ETES, and PTES were included in separate gel formulations. As above, all sample types were prepared in triplicate at identical tracer concentrations for each tracer type. Tracer ions were prepared in BG-11 medium prior to mixing with hydrolyzed gel precursors to form gel samples. Tracers included Ni^{2+}, methyl orange, copper(II)EDTA, and potassium dichromate, included in gel samples at concentrations of 300 mM, 1.25 mM, 200 mM, and 2.42 mM, respectively. For comparison, gels prepared from aqueous precursors were also included in this sample set. Sample set 2 included 27 different sample types prepared in triplicate for a total of 81 samples.

The aqueous-derived gels were prepared by combining 8.0 mL 40% sodium silicate solution with 57.6 mL deionized water, 1.85 mL hydrochloric acid (1.0 M), and 23.2 g ion exchange resin (Amberlite™ IR-120(H), Alfa Aesar, Ward Hill, MA) and stirring vigorously with a magnetic stir bar for approximately 2 h at room temperature. The ion exchange resin was then sieved out, and the solution was vacuum filtered. 3.0 mL of this aqueous precursor was combined with 5.0 mL additional liquid, appropriate parts BG-11 medium and tracer stock solution, in a 35 mm Petri dish. This yielded a gel with a final silica content of 187:1, molar ratio water to silica, and identical tracer concentrations to the alkoxide-derived samples described above.

2.3. Diffusion measurements

Diffusion was measured by placing tracer-impregnated gels in 240 mL of continuously stirred deionized water, and monitoring the concentration of the tracer in the water as a function of time. The concentration of Ni^{2+} was monitored spectrophotometrically at a wavelength of 395 nm using a Spectronic Genesys 10 Bio UV–Vis spectrophotometer (Thermo Scientific, Waltham, MA), as performed elsewhere [27,28]. The diffusion of the other tracers was measured similarly, with the concentration of Cu(II)EDTA measured at 732 nm, dichromate at 372 nm, and methyl orange at 466 nm. Calibration curves were developed to ensure resolution of the spectrophotometric measurement of concentration for each tracer and linear behavior (Beer's Law) over the concentration ranges studied (data not shown).

Samples were analyzed approximately 24 h after preparation. During analysis, a 1.0 mL aliquot was periodically removed for concentration measurements and returned to the sealed reaction vessel. Experiments were terminated at 3 h, at which point the concentration of tracer was approximately 40–60% of equilibrium for all samples examined. From the time series of concentration data, the diffusion coefficient for the tracer ion in the gel (D_{gel}) was calculated for each sample.

2.4. Calculation of diffusion coefficients

Diffusion coefficients were calculated for each sample type using an analytical solution to Fick's Second Law describing ideal one-dimensional diffusion from a finite slab into a well stirred sink [29,30], used in similar form elsewhere to estimate diffusion of Ni^{2+} in silica gel [27,28,31]. Shown in Eq. (1), the solution equating the ratio of concentration at time t to the equilibrium concentration takes the form of a trigonometric series where l is the thickness of the gel and D_{gel} is the diffusion coefficient (assumed to describe diffusion of the tracer within the gel as this is the rate limiting process as the concentration of the tracer increases in the well-stirred sink). The series was expanded to five terms for calculating D_{gel}; higher order expansion did not alter the results to two significant figures (data not shown).

$$\frac{C_t}{C_{\mathbb{N}}} = 1 - \sum \frac{8}{(2n+1)^2\pi^2} \exp\left[\frac{-D_{gel}(2n+1)^2\pi^2 t}{l^2}\right] \quad (1)$$

With sample set 1, D_{gel} was calculated by ANOVA using SAS v9.2 (SAS Institute, Inc., Cary, NC) and also by the Solver add-in of Microsoft Excel (Microsoft Corp., Redmond, WA). With Solver, the objective function minimized the sum of squared variance between the analytical solution and the raw experimental data by altering the value of D_{gel}. No statistically significant difference was found between the two methods (data not shown). After this comparison, Solver was used to calculate D_{gel} for sample set 2.

2.5. Transmission electron microscopy

We used transmission electron microscopy (TEM) in an attempt to provide a description of gel structure. Samples were prepared as described above with a TEOS precursor at a hydrolysis ratio of 20:1, acid ratio of 0.005 and dilution ratio of 100:1. Gels contained cells of *Synechocystis* at a concentration of approximately 1×10^8 cells/mL. Samples were prepared in 35 mm Petri dishes, as described above. Gels were manually sliced with a razor blade, flash frozen in liquid nitrogen and prompted imaged in an FEI Titan FEG-TEM (FEI Company, Hillsboro, OR) at the Center for Advanced Materials Characterization in Oregon (CAMCOR; University of Oregon, Eugene, OR) with assistance from CAMCOR staff.

3. Results

Diffusion coefficients, D_{gel}, for Ni^{2+} were calculated for all samples in sample set 1 using Eq. (1) and the results are listed in Table 1, by formulation chemistry with sample ID and 95% confidence intervals. Sample 1 excepted, the calculated values of D_{gel} fell between 1.37×10^{-10} m^2 s^{-1} and 6.27×10^{-10} m^2 s^{-1}, or approximately 14–63% of the value of D expected for Ni^{2+} in unconfined aqueous solution of approximately 1×10^{-9} m^2 s^{-1} [27]. As shown in Table 1 and Fig. 2a, sample 1 in particular ($D_{gel} = 9.05 \times 10^{-10}$ m^2 s^{-1}), but also samples 7, 19, 24, 34, and 44, are significantly above a mean where the other samples are clustered and generally have overlapping error bars. The mean for the entire sample set is 2.90×10^{-10} m^2 s^{-1} ($\pm 4.25 \times 10^{-11}$ m^2 s^{-1}). Excluding the six samples mentioned above, the remaining samples are clustered at a mean of approximately 2.42×10^{-10} m^2 s^{-1} ($\pm 1.88 \times 10^{-11}$ m^2 s^{-1}). Samples 13, 14, and 29 gelled prematurely

Table 1
D_{gel} values for sample set 1 (Ni^{2+} tracer). "95% CI" = 95% confidence interval.

Gel type	Water ratio	Acid ratio	Dilution ratio	D_{gel} ($m^2\ s^{-1}$)	95% CI	Sample ID
TEOS	4	0.005	10	9.05E−10	2.02E−10	1
			20	3.52E−10	9.95E−11	2
			40	2.17E−10	1.60E−11	3
			60	2.72E−10	2.90E−11	4
			80	2.53E−10	3.00E−11	5
			100	4.02E−10	1.02E−10	6
		0.01	10	5.36E−10	3.92E−11	7
			20	2.58E−10	8.71E−11	8
			40	2.00E−10	1.40E−11	9
			60	2.09E−10	2.00E−11	10
			80	1.81E−10	1.60E−11	11
			100	3.32E−10	9.30E−11	12
		0.02	10	–	–	13
			20	–	–	14
			40	3.06E−10	6.60E−11	15
			60	1.76E−10	1.05E−11	16
			80	1.55E−10	1.40E−11	17
			100	2.35E−10	1.70E−11	18
	10	0.005	20	5.67E−10	1.76E−10	19
			40	2.23E−10	1.80E−11	20
			60	2.18E−10	2.90E−11	21
			80	2.20E−10	1.90E−11	22
			100	1.94E−10	1.70E−11	23
		0.01	20	5.28E−10	9.9E−11	24
			40	3.78E−10	1.16E−10	25
			60	2.79E−10	4.60E−11	26
			80	2.80E−10	6.95E−11	27
			100	1.74E−10	2.10E−11	28
		0.02	20	–	–	29
			40	2.66E−10	4.20E−11	30
			60	2.47E−10	5.05E−11	31
			80	1.44E−10	1.65E−11	32
			100	2.63E−10	2.15E−11	33
	20	0.005	40	6.27E−10	2.01E−10	34
			60	2.32E−10	2.90E−11	35
			80	2.39E−10	2.85E−11	36
			100	2.27E−10	1.65E−11	37
			120	2.53E−10	8.73E−11	38
		0.01	40	2.55E−10	3.45E−11	39
			60	2.12E−10	1.55E−11	40
			80	1.74E−10	8.50E−12	41
			100	2.06E−10	1.55E−11	42
			120	2.42E−10	1.12E−10	43
		0.02	40	4.60E−10	3.10E−11	44
			60	2.08E−10	8.50E−12	45
			80	3.04E−10	5.30E−11	46
			100	3.09E−10	2.85E−11	47
			120	1.37E−10	2.20E−11	48

while the precursor was hydrolyzing, due to high precursor and acid catalyst concentrations.

Calculated D_{gel} values for Ni^{2+}, Cu(II)EDTA, methyl orange, and dichromate in sample set 2 are shown in Fig. 2b by gel environment with 95% confidence intervals. As can be seen in this figure, while D_{gel} values vary between tracer compounds, values for the same tracer are generally very similar, often with over lapping confidence intervals among the various gel environments.

Fig. 3a shows a ratio of D_{gel} to D in unconfined aqueous solution, D_{sol}, for the four selected tracers in the seven gel environments. D_{sol} values are shown in Table 2, as well as estimated maximum molecular dimensions for each of the tracers and those estimated for carbonate, bicarbonate, and dissolved CO_2, for comparison. D_{gel} values for these carbon species were estimated using linear correlations calculated from the results of the four tracers (see below). Molecular dimension estimates for all compounds listed in Table 2 were calculated with Spartan 4 (Wavefunction, Inc., Irvine, CA). As shown, the diffusion of the larger tracers, methyl orange and Cu(II)EDTA, are significantly hindered by encapsulation in silica gel, with D_{gel} consistently less than 5% of D_{sol} for methyl orange and less than 15% of D_{sol} for Cu(II)EDTA. There was more variability with the smaller tracers, Ni^{2+} and dichromate, but in some cases D_{gel} exceeded 30% of D_{sol}.

Table 3 lists linear correlations between D_{gel} values and estimated molecular dimensions for each compound and each gel type. Generally, a strong linear inverse correlation between tracer size and the magnitude of its corresponding diffusion coefficient was shown in most instances. One notable exception was in the PTES environment where Ni^{2+} has a surprisingly small D_{gel} value, reducing the strength of the correlation and indicating other interactions are affecting diffusion. Fig. 3b shows the linear correlation between diffusion coefficient and tracer size using mean D_{gel} values for each tracer across gel environments.

Fig. 4 shows three TEM images of an example gel containing encapsulated cyanobacterial cells (right panel). Although flash freezing and subsequent evaporation within the TEM chamber likely caused some changes to the gel structure and prevented high resolution imaging, it is clear from the images that the bulk of the structure is composed of particles on the order of 10–50 nm in diameter. Furthermore, the pore distribution appears bimodal,

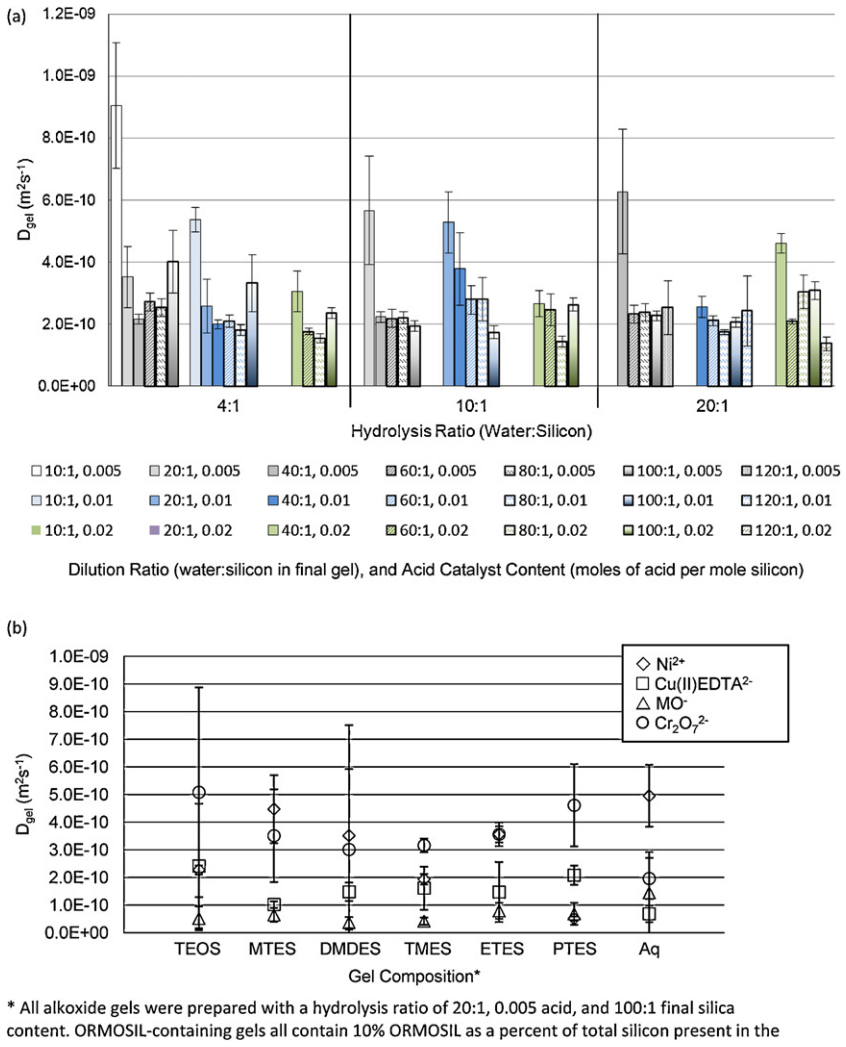

Fig. 2. (a) D_{gel} values for sample set 1 (Ni^{2+} tracer). (b) Shows D_{gel} values for sample set 2, for all four tracers at each gel composition. Error bars represent 95% confidence intervals.

containing some mesopores on the order 50–100 nm in diameter (left and center panels) and a more typical fine pore structure generally <10 nm in diameter. Also worth noting in the right panel, showing an interface between the gel and an encapsulated cell, is evidence that the gel makes close contact with the cell surface. Presumably, the fine pore structure is the dominant feature controlling diffusion. It is unclear if the necking clearly visible between the particles is present in the hydrated gels or occurred during flash freezing and imaging.

4. Discussion

4.1. Sample set 1: processing space and Ni^{2+}

The hydrolysis ratio (i.e. water present during the acid-catalyzed hydrolysis of the precursor) was varied at 4:1, 10:1, and 20:1, water to silicon molar ratio. The 4:1 gels, using a stoichiometric amount of water during hydrolysis, were used as a baseline composition to contrast with 10:1 and 20:1 gels, where hydrolysis was

Table 2
A comparison of largest molecular dimensions, D_{gel} values, D_{sol} values, D_{gel}/D_{sol} for each tracer, and values estimated for bicarbonate, carbonate, and dissolved CO_2.

Compound	Ion of interest (tracer)	Molecular radius (largest dimension, Å) [a]	D_{gel} (pure TEOS gel; $\times10^{-10}$ m^2 s^{-1})	D_{sol} (unconfined solution; $\times10^{-10}$ m^2 s^{-1})	D_{gel}/D_{sol}
Nickel chloride	Ni^{2+}	5.4	2.27	13.2[39]	0.172
Sodium Cu(II)EDTA	$[Cu(II)EDTA]^{2-}$	6.8	2.41	15.4[40]	0.156
Methyl orange	$C_{14}H_{14}N_3O_3S^-$	7.8	0.514	14.0[41]	0.037
Potassium dichromate	$Cr_2O_7^{2-}$	5.5	5.08	13.9[42]	0.365
Bicarbonate	HCO_3^-	2.3	3.96[b]	11.85[39]	0.334
Carbonate	CO_3^{2-}	3.8	4.10[b]	11.5[43]	0.357
Carbon dioxide	CO_2(aq)	3.5	4.11[b]	19.1[39]	0.215

[a] Estimates based on calculations performed using Spartan 4.
[b] Estimate based on linear extrapolation from experimental data for diffusion of the four tracers from gels composed of pure TEOS.

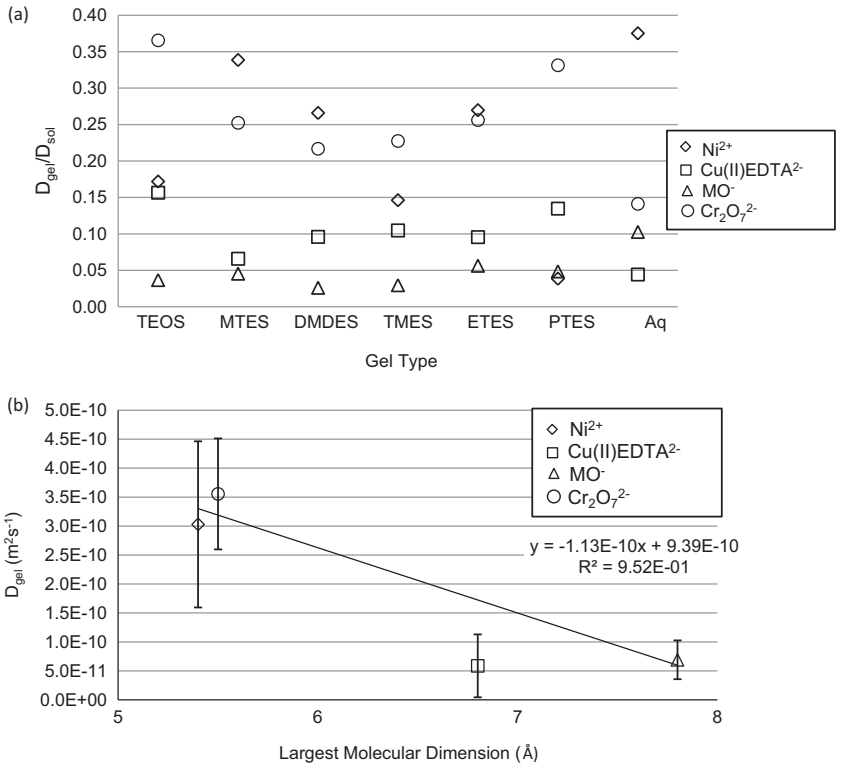

Fig. 3. (a) D_{gel}/D_{sol} for all four tracers at each gel composition. (b) Mean D_{gel} versus tracer size with linear regression and R^2 value. Error bars represent 95% confidence intervals.

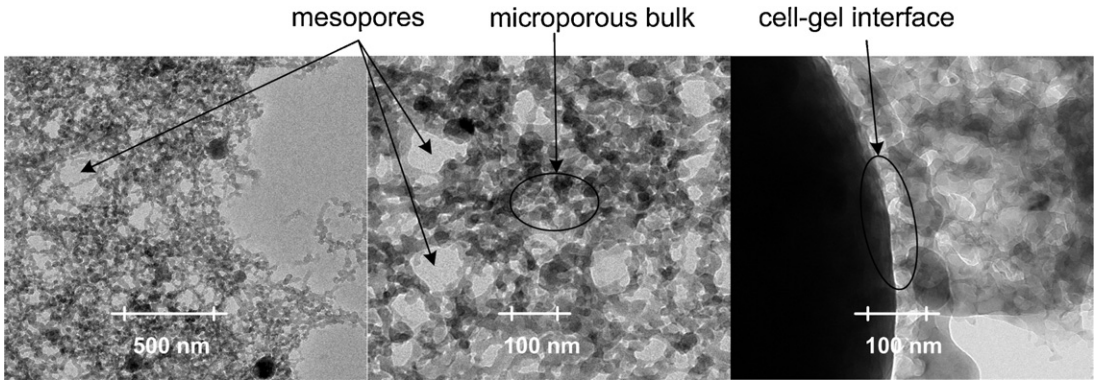

Fig. 4. TEM images of an alkoxide-derived gel containing cells of *Synechocystis*.

Table 3
Linear correlations for D_{gel} values and tracer size in all seven gel formulations, with R^2 values, predicted *x*-intercepts (hypothetically, the size at which a tracer would effectively be immobilized in the gel), and 1-h characteristic diffusion length ($\sqrt{Dt}$) for CO_2 in each gel formulation.

Gel type	Linear correlation (x = molecular dimension; $y = D_{gel}$)	R^2	*X*-intercept (Å)[b]	1-H CO_2 diffusion length ($\sqrt{Dt}$; mm)[c]
Pure TEOS	$y = -1.25E{-}10x + 1.05E{-}9$	0.575	8.4	1.5
10% MTES	$y = -1.55E{-}10x + 1.23E{-}9$	0.896	7.9	1.3
10% DMDES	$y = -1.25E{-}10x + 1.01E{-}9$	0.987	8.1	1.4
10% TMES	$y = -8.58E{-}11x + 7.25E{-}10$	0.758	8.4	1.2
10% ETES	$y = -1.23E{-}10x + 1.02E{-}9$	0.970	8.3	1.5
10% PTES	$y = -6.82E{-}11x + 6.31E{-}10$	0.169	9.3	1.2
	($y = -1.72E{-}10x + 1.40E{-}9$)[a]	(0.992)[a]	(8.1)	(2.2)
Aqueous	$y = -1.07E{-}10x + 9.08E{-}10$	0.428	8.5	1.4

[a] Linear correlation excluding Ni^{2+}.
[b] *X*-intercept of the shown linear correlations, where D_{gel} would theoretically reach 0, completely confining the encapsulated component within the gel.
[c] Diffusion length over a 1-h period, assuming a molecular dimension for CO_2 of 3.5 Å (calculated with Spartan 4) and diffusion coefficients estimated from the linear correlations shown in column 2.

expected to be mostly complete due to excess water [21,23,32]. The rationale for including these samples was to examine gels where cross-linking, and therefore overall density, might be reduced due to bonding sites being occupied by unhydrolyzed alkoxide groups. This effect was most dramatic in the low silica content samples (a dilution ratio of 100:1). Samples 6 and 12 were extremely soft and fragile, deteriorating upon slight mechanical agitation at the conclusion of the experimental analysis. Preparing samples with a dilution ratio of 120:1 was not possible with a 4:1 hydrolysis ratio because gelation simply did not occur, likely due to poor hydrolysis of the precursor. As a consequence of this mechanical frailty, the calculated D_{gel} values of 4.02 and 3.32×10^{-10} m^2 s^{-1}, respectively, were higher than most other samples. This was not interpreted as an improvement in diffusion, but the result of ablation of the gel into the stirred water of the reaction vessel. Mechanical strength is necessary for any immobilized cell reactor based on this chemical system, so limiting the amount of water during hydrolysis is not recommended.

Both the 10:1 and 20:1 systems are viable options for biological encapsulation. Hydrolysis is expected to be nearly complete [23], allowing for the removal of alcohol, and observed differences in diffusion behavior were insignificant. The 4:1 system, by contrast, is not expected to be a good candidate for biological encapsulation because hydrolysis is incomplete upon gelation. In addition to being mechanically unstable, subsequent hydrolysis within the gel could yield potentially cytotoxic concentrations of alcohol.

Although acid catalyst content is known to impact the hydrolysis rate [33–37], acid concentration did not have a significant effect on the diffusion of Ni^{2+} in this work. Presumably, the macroscopic measurement of the diffusion of Ni^{2+} did not provide the resolution to identify differences between the gels prepared with differing acid ratios over the range examined. For biological encapsulation, it is therefore advisable to use the minimal amount of acid that will catalyze complete hydrolysis in a reasonable time, minimizing additional stress on the biological component. However, some acid is necessary to catalyze hydrolysis because the time required for hydrolysis in the absence of acid is so long as to be impracticable for most biological encapsulation applications.

The dilution ratio, covering a range of approximately 2.5–32 wt.% silica in the final gels, also had little effect on the diffusion rate of Ni^{2+} over the composition range studied in this investigation. It was expected that lower silica content would create a more open, less dense structure that would lead to faster diffusion, but this was not observed (Fig. 2a). The exceptions included the low hydrolysis ratio and high dilution ratio samples discussed previously (samples 6 and 12) and samples where silica content was high, including samples 1, 7, 13, 14, 19, 24, 29, and 34 (Table 1). Samples 13, 14, and 29 could not be synthesized by the protocols of the current investigation because the sol gelled during initial hydrolysis as a result of high silica content, limiting water, and high acid content which catalyzed condensation. Samples 1, 7, 19, 24, and 34 were successfully prepared but exhibited significant syneresis, which artificially augmented the diffusion process by expelling liquid phase from the gel. All three replicates of each sample type shrank by as much as 10%, which would place considerable mechanical stress on an encapsulated biological component.

That the Ni^{2+} diffusion coefficients measured in this study did not vary significantly over such a range of silica content implies that silica content can be adjusted widely to suit the application with minimal change in diffusion transport of small cations. Since sample set 1 examined diffusion of only Ni^{2+}, the conclusions pertaining to these experiments are limited to ions or molecules of a comparably small size and charge (hydrated Ni^{2+} in solution, in octahedral coordination, is estimated to have an effective diameter on the order of 1 nm). Therefore, diffusion of larger, perhaps biologically relevant molecules may be hindered, warranting the inclusion of sample set 2.

4.2. Sample set 2: ORMOSILs and tracer size

ORMOSILs contain unhydrolyzable carbon–silicon bonds which incorporate organic functional groups into the gel matrix. This second investigation included varying degrees of simple alkyl side groups, including methyl alkoxysilanes MTES, DMDES, and TMES, as well as a singly substituted ETES and PTES. The effects of using such additives are threefold. First, the alkyl groups cause inductive and steric hindrance to acid catalyzed hydrolysis [33]. Second, these alkyl groups occupy bonds that would otherwise be occupied by oxygen bridges, loosening the structure of the gel and providing some flexibility [37]. There is an optimal amount of ORMOSIL that can be added, however, as the lack of bridging will eventually degrade a flexible gel to a viscous liquid as the number of organic side groups increases [38]. Lastly, alkyl groups are hydrophobic, in contrast to hydrophilic hydroxyl groups, altering the interfacial energy between the solid matrix and liquid phase.

Fig. 2b shows the calculated diffusion coefficients of tracers in gels containing 10 mol.% ORMOSIL. At the same 10 mol.%, these ORMOSILs contributed one methyl, ethyl, or propyl group, or two or three methyl groups per silicon, which occupied 2.5%, 5%, and 7.5% of potential bonding sites. Since drying was not performed, the dominant effect was expected to be reduced condensation and cross-linking after gelation, increasing the flexibility of the gel and avoiding syneresis. Consistent with this expectation, no shrinkage was observed in gels containing ORMOSILs.

Sample set 2 also included gels derived from aqueous precursors which have no organic groups bound to silicon and no alcohol, so they may be more biocompatible than alkoxide alternatives. Furthermore, the sol preparation employs lower silicon concentrations, so condensation prior to gelation is reduced, providing the ability to synthesize stable gels with lower silica content than alkoxide-derived gels.

With the larger tracers, Cu(II)EDTA and methyl orange, ORMOSILs had no significant effect on D_{gel}. The dominant effect appeared to be the size of the diffusing molecule, not the hydrophobicity of the gel surface (Fig. 3b). It is plausible and certainly likely that surface interactions were occurring, but were of secondary importance compared to confinement by the pore structure (shown in Fig. 4). Diffusion of dichromate was similarly unaffected by the presence of ORMOSILs despite its comparatively smaller size. However, this is in contrast to the diffusion of Ni^{2+}, which was significantly slower in some gel chemistries, including TEOS, TMES, and particularly PTES (Fig. 2b). In contrast, D_{gel} for Ni^{2+} in aqueous gels was larger by comparison to the other tracers in the same chemistry.

It is difficult to reconcile these differences with any one explanation. Ni^{2+} was the only cationic tracer used in this study, so there may be an electrostatic interaction occurring with this ion that is not occurring with the other species. However, if a strong surface interaction was responsible for the hindered diffusion of Ni^{2+} from pure TEOS gels, which are presumably hydrophilic with hydroxyl surface groups, one would expect a similar effect in aqueous gels with similarly hydrophilic character. The opposite was observed, diffusion occurred more quickly from aqueous gels, which is not consistent with a purely electrostatic interaction. It is also unclear why Ni^{2+} would diffuse more slowly from ORMOSIL-containing gels. If anything, one might expect diffusion to be increased by the combination of the ORMOSILs opening the pore structure and the hydration shell around the Ni^{2+} ion having a repulsive electrostatic interaction with the hydrophobic alkyl surface groups. Therefore, it remains unknown what caused these observed inconsistencies in the diffusion of Ni^{2+}.

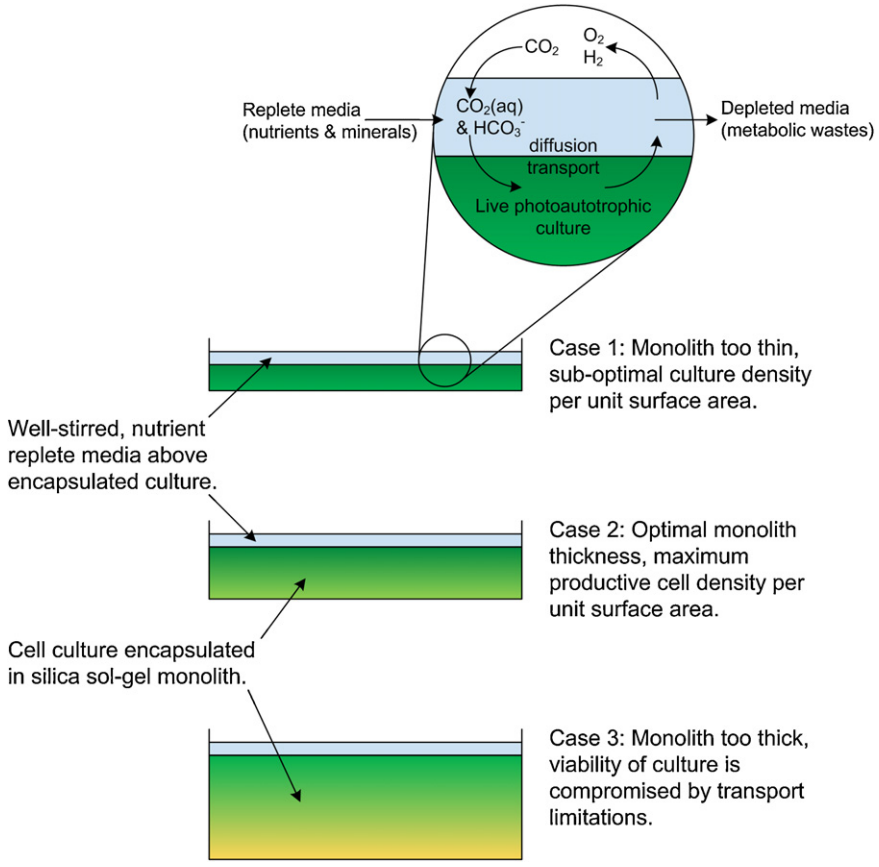

Fig. 5. An illustration of how diffusion is relevant to optimal gel geometry (not to scale).

The size of the diffusing molecule appeared to be the dominant factor in determining diffusion rates, not the hydrophobicity as altered by the use of ORMOSILs. Although the ORMOSILs did not affect a significant change in diffusion rates in most instances, the fact that no syneresis was observed does support the conclusion that these compounds increase the flexibility of the gel and may therefore be used to better tailor gel chemistry for biological encapsulation with minimal detrimental impact on the diffusion of small molecules.

4.3. Implications for encapsulation

Calculated D_{gel} values and molecular dimensions were used to establish a linear correlation between diffusion coefficients and the size of the tracer (Fig. 3b; Table 3). This correlation was then used to estimate D_{gel} in a TEOS gel for carbonate, bicarbonate, and dissolved CO_2 (Table 2). In the case of encapsulating viable phototrophs like cyanobacteria, adequate transport of carbon species is critical to support carbon fixation. If encapsulated phototrophs are to be used as a platform for the conversion of atmospheric CO_2 into value-added products, this transport will likely be the limiting process.

Using the linear correlation established above, D_{gel} for the three carbon compounds in TEOS gel are on the order of approximately 4.0×10^{-10} m^2 s^{-1}, or approximately 35% of D_{sol} for the carbonate species and 21% of D_{sol} for dissolved CO_2. This results in a 1-h characteristic diffusion length, $\sqrt{Dt}$, on the order of 1.5 mm. In order to optimize encapsulation geometry, in this case for maximal utilization of available light and CO_2, it is important to make the gel thick enough to fully leverage light and cell density, yet not so thick that cells within the monolith are unproductive. Conversely, if the gel is too thin, the system may not be fully utilizing either available light or available CO_2 (Fig. 5). Although not yet optimized, a previous investigation documented minimal degradation in photosynthetic efficiency of encapsulated cultures of *Synechocystis* encapsulated in aqueous- and TEOS-derived gels that were 5 mm thick over 8 weeks [19]. However, cells in gels 10 mm thick display visible signs of chlorosis near the bottom of the monolith (data not shown), indicating a clear threshold in transport limitations on the order of millimeters. For diffusion of larger molecules, the optimal geometry is likely on the order of a single millimeter or 100s to 10s of microns.

5. Conclusion

Four ionic tracers, including Ni^{2+}, Cu(II)EDTA, methyl orange, and dichromate, were used to investigate diffusion from wet silica sol–gel monoliths. In sample set 1, hydrolysis ratio, acid ratio, and dilution ratio ranges were selected based on relevance to biological encapsulation and explored in a factorial design with Ni^{2+} as the tracer. Sample set 2 explored diffusion of all four tracers in gels prepared with TEOS and aqueous precursors, as well as gels containing 10% of numerous ORMOSILs. D_{gel} was calculated for all sample types using an analytical solution to Fick's Second Law. There was surprisingly little variation over the process space. The mean across the entire processing space included in sample set 1 was approximately 2.90×10^{-10} m^2 s^{-1}. Excluding six outlier samples which displayed significant syneresis, the mean was 2.42×10^{-10} m^2 s^{-1}.

Sample set 2 indicated that the tracer size and not gel hydrophobicity was the primary determinant of changes in diffusion rates. A strong linear inverse correlation was found between tracer size and the magnitude of D_{gel}. However, the correlation was less strong in some gel chemistries, particularly gels containing PTES, due to inconsistent diffusion of Ni^{2+}. It is unclear what kinds of surface interactions may be occurring to cause these discrepancies.

Finally, based on correlation with the tracers used in this investigation, it has been determined that adequate diffusion of carbon species relevant to supporting active phototrophic organisms likely occurs in gels up to a few millimeters thick. TEM imaging indicated that the gel does approach the surface of the cell and likely constrains diffusion similarly to the bulk of the gel monolith. These results support the notion that silica sol–gel formulations may be optimized for a given biological entity of interest with manageable impact to the diffusion of small ions and molecules. However, as the size of the diffusing compound increases, diffusion may become limiting and thus must be considered when optimizing gel geometry.

Acknowledgments

This material is based upon work supported by the National Science Foundation under Grant No. 0829199-CBET and the Air Force Office of Scientific Research, Proposal No. 08NL208. The authors would like to thank the staff at CAMCOR for TEM assistance, Tia Gabalita for assistance with statistical analysis, and Kelsey Baker, Kelsey Ward, Patricia Choi, Rebecca Miller, and Anna Leitschuh for laboratory assistance.

References

[1] A.C. Pierre, Biocatal. Biotransform. 22 (2004) 145–170.
[2] H. Bottcher, U. Soltmann, M. Mertig, W. Pompe, J. Mater. Chem. 14 (2004) 2176–2188.
[3] D. Avnir, T. Coradin, O. Lev, J. Livage, J. Mater. Chem. 16 (2006) 1013–1030.
[4] C.F. Meunier, P. Dandoy, B.-L. Su, J. Colloid Interface Sci. 342 (2010) 211–224.
[5] S.Y. Gadre, P.I. Gouma, J. Am. Ceram. Soc. 89 (2006) 2987–3002.
[6] R. Gupta, N.K. Chaudhury, Biosens. Bioelectron. 22 (2007) 2387–2399.
[7] V. Kandimalla, V. Tripathi, H. Ju, CRC Cr. Rev. Anal. Chem. 36 (2006) 73–106.
[8] M. Kato, Kumiko Sakai-Kato, Toshimasa Toyo'oka, J. Sep. Sci. 28 (2005) 1893–1908.
[9] N. Koone, Y. Shao, T.W. Zerda, J. Phys. Chem. 99 (1995) 16976–16981.
[10] N. Koone, T. Zerda, J. Sol–Gel Sci. Technol. 8 (1997) 883–887.
[11] W.J. Elferink, B.N. Nair, R.M.d. Vos, K. Keizer, H. Verweij, J. Colloid Interface Sci. 180 (1996) 127–134.
[12] B.N. Nair, W.J. Elferink, K. Keizer, H. Verweij, J. Colloid Interface Sci. 178 (1996) 565–570.
[13] P.J. Davis, C.J. Brinker, D.M. Smith, J. Non-Cryst. Solids 142 (1992) 189–196.
[14] Y. Jiang, Z. Wu, L. You, H. Xiang, Colloids Surf. B. Biointerfaces 49 (2006) 55–59.
[15] J. Kunetz, L. Hench, J. Am. Ceram. Soc. 81 (1998) 877–884.
[16] S. Satoh, I. Matsuyama, K. Susa, J. Non-Cryst. Solids 190 (1995) 206–211.
[17] A. Dewitt, K. Herwig, S. Lombardo, Adsorption 11 (2005) 491–499.
[18] D.J. Dickson, C.J. Page, R.L. Ely, Int. J. Hydrogen Energy 34 (2009) 204–215.
[19] D.J. Dickson, R.L. Ely, Appl. Microbiol. Biotechnol. 91 (2011) 1633–1646.
[20] R. Aelion, A. Loebel, F. Eirich, J. Am. Chem. Soc. 72 (1950) 5705–5712.
[21] C.J. Brinker, K.D. Keefer, D.W. Schaefer, C.S. Ashley, J. Non-Cryst. Solids 48 (1982) 47–64.
[22] M.F. Bechtold, R.D. Vest, J. Louis Plambeck, J. Am. Chem. Soc. 90 (1968) 4590–4598.
[23] J.C. Pouxviel, J.P. Boilot, J.C. Beloeil, J.Y. Lallemand, J. Non-Cryst. Solids 89 (1987) 345–360.
[24] L.W. Kelts, N.J. Armstrong, J. Mater. Res. 4 (1989) 423–433.
[25] M.P.J. Peeters, T.N.M. Bernards, M.J. Van Bommel, J. Sol–Gel Sci. Technol. 13 (1998) 71–74.
[26] M.M. Allen, J. Phycol. 4 (1968) 1–4.
[27] R. Takahashi, S. Sato, T. Sodesawa, Y. Kamomae, Phys. Chem. Chem. Phys. 2 (2000) 1199–1204.
[28] R. Takahashi, S. Sato, T. Sodesawa, H. Nishida, Phys. Chem. Chem. Phys. 4 (2002) 3800–3805.
[29] J. Crank, The Mathematics of Diffusion, second ed., Oxford University Press, Bristol, UK, 1975.
[30] P.L. Ritger, N.A. Peppas, J. Control. Release 5 (1987) 23–36.
[31] R. Takahashi, S. Sato, T. Sodesawa, H. Nishida, J. Ceram. Soc. Jpn. 109 (2001) 840–845.
[32] J.C. Pouxviel, J.P. Boilot, J. Non-Cryst. Solids 94 (1987) 374–386.
[33] C.J. Brinker, G.W. Scherer, Sol–Gel Science, Academic Press, Inc., San Diego, CA, 1990.
[34] E.J.A. Pope, J.D. Mackenzie, J. Non-Cryst. Solids 87 (1986) 185–198.
[35] R.A. Assink, B.D. Kay, Annu. Rev. Mater. Sci. 21 (1991) 491–513.
[36] L.C. Klein, Annu. Rev. Mater. Sci. 15 (1985) 227–248.
[37] N.K. Raman, S. Wallace, C.J. Brinker, Mater. Res. Soc. Symp. Proc. 435 (1996) 6.
[38] R.H. Glaser, G.L. Wilkes, J. Non-Cryst. Solids 113 (1989) 73–87.
[39] W.M. Haynes, CRC Handbook of Chemistry and Physics, CRC Press/Taylor & Francis, Boca Raton, FL, 2011.
[40] D.G. Leaist, L. Hao, J. Chem. Soc. Faraday Trans. 90 (1994) 133–136.
[41] L.D. Backer, G. Baron, J. Chem. Technol. Biotechnol. 59 (1994) 297–302.
[42] N. Iadicicco, L. Paduano, V. Vitagliano, J. Chem. Eng. Data 41 (1996) 529–533.
[43] D.G. Leaist, R. Noulty, Can. J. Chem. 63 (1985) 2319–2323.